

## A new mechanism for stability loss from a heteroclinic cycle

Claire M. Postlethwaite<sup>†</sup>

Department of Mathematics, University of Auckland, Private Bag 92019, Auckland,  
New Zealand

(May 20, 2010)

Asymptotically stable robust heteroclinic cycles can lose stability through resonance or transverse bifurcations. In a transverse bifurcation, an equilibrium in the cycle undergoes a local bifurcation, causing a change in stability. A resonance bifurcation is a global phenomenon, determined by an algebraic condition on the eigenvalues, and is generically accompanied by the birth or death of a long-period periodic orbit. In this paper we demonstrate a new mechanism causing loss of stability, which is neither resonant nor transverse in the usual sense. The location of the instability is determined by an algebraic condition on the eigenvalues, but the instability occurs in a transverse direction. Furthermore, after the bifurcation, when the cycle is unstable, open sets of trajectories are seen to initially approach the network for an extended period, before moving away in the unstable direction. This should serve as a warning to all those doing numerics near heteroclinic cycles who deduce the cycle is stable merely because trajectories are observed to initially approach the cycle.

### 1 Introduction

Heteroclinic trajectories between saddle-like invariant sets are of great interest in dynamical systems. They can act as organising centres for many types of non-trivial behaviour, including intermittency and chaotic dynamics. In generic systems, heteroclinic orbits are of high codimension, but it is well known that in systems containing invariant subspaces they can exist for open sets of parameter values, that is, they are of codimension zero, and are referred to as ‘robust’ [1–3]. Three situations in which such invariant subspaces can arise are (i) due to equivariance with respect to a symmetry group [4, 5], (ii) modelling assumptions such as the permanence of death in Lotka–Volterra-type models of population dynamics [6–8] also seen in mod-

---

<sup>†</sup> c.postlethwaite@math.auckland.ac.nz

els of neural decision-making processes [9–12], and (iii) structural restrictions such as the coupled cell structures investigated recently by Aguiar et al. [13].

It has long been a goal of many researchers in dynamical systems to compute a general necessary and sufficient condition for the asymptotic stability of heteroclinic cycles [4, 5, 14, 15]. However, the results have turned out to be much more subtle than was first thought, and examples have continued to appear showing that previously given conditions, although sufficient, are not in fact necessary [5, 16]. Alongside stability computations come studies of the bifurcations which occur when stability conditions are broken. Until now, studies of bifurcations from robust heteroclinic cycles have concentrated on resonant bifurcations [15, 17–19] and transverse bifurcations [20]. Both bifurcations are from a cycle which is initially asymptotically stable. In a transverse bifurcation, a local bifurcation causes an eigenvalue of one of the equilibria in the cycle to change sign. This can result in a bifurcating periodic orbit or heteroclinic cycle, depending on the specific situation. After the bifurcation, the heteroclinic cycle is no longer asymptotically stable, but it may still have strong attractivity properties, as discussed further below. A resonance bifurcation is a global phenomena, determined by an algebraic condition on the eigenvalues, and generically accompanied by the birth or death of a long-period periodic orbit. After a resonance bifurcation, we would normally expect the basin of attraction of the cycle to have measure zero.

Heteroclinic cycles can have strong attractivity properties even if they are not asymptotically stable. One commonly observed type of stability is *essential asymptotic stability*, introduced first by Melbourne [21]. Here the set of points in the basin of attraction of the cycle has a measure which increases in some sense as the cycle is approached. This often occurs if a cycle has a small, but positive, transverse eigenvalue, for instance, shortly after a transverse bifurcation.

In this paper, we discuss a mechanism by which a heteroclinic cycle, which is essentially asymptotically stable, can lose stability. This mechanism is neither a resonant nor a transverse bifurcation, although it has properties similar to both. The condition for the instability is given by an algebraic condition on the eigenvalues, as in a resonance bifurcation. However, the loss of stability occurs in a transverse direction, and does not appear to be accompanied by the birth or death of a periodic orbit or other object. This is in contrast to generic bifurcations, in which stability change is usually accompanied by the

creation or disappearance of some sort of dynamical structure.

Furthermore, after the loss of stability, the set of points which asymptote onto the cycle is of measure zero, but open sets of initial conditions arbitrarily close to the cycle initially approach the heteroclinic cycle before moving away. This could have the effect of causing misleading numerics in simulations of trajectories near heteroclinic cycles. Numerical simulations near robust heteroclinic cycles can be difficult when coordinates become very small as invariant subspaces are approached. Thus it is often assumed that in a numerical simulation, a trajectory approaching a heteroclinic cycle will only continue to do so until the numerical error is larger than the distance of the trajectory from the subspace. However, trajectories near a cycle which is unstable in the manner described in this paper will have a similar behaviour — that is, they initially approach the cycle, but after some time they start to move away. Hence what may appear to be a numerical artifact near a stable cycle may actually indicate an unstable heteroclinic cycle.

This paper is arranged as follows. In section 2 we first give some preliminaries and definitions regarding the structure of robust heteroclinic cycles. We then discuss the type of heteroclinic cycle we are particularly interested in for the purposes of this paper, and describe the construction of Poincaré maps, the standard method of analysing the stability of heteroclinic cycles. In section 3 we analyse the Poincaré maps, and describe the new mechanism for loss of stability. Our method of analysis involves reducing the two-dimensional Poincaré maps to the study of a one-dimensional map acting on parameters within a family of curves. In section 4 we give a numerical example, showing the behaviour of trajectories before and after the loss of stability, and in section 5 we conclude.

## 2 Robust heteroclinic cycles

### 2.1 Definitions and Preliminaries

We consider continuous-time dynamical systems in the form of  $\Gamma$ -equivariant ODEs:

$$\dot{x} = f(x), \quad x \in \mathbb{R}^n, \quad (1)$$

where  $\Gamma \subset \mathbf{O}(n)$  is a finite Lie group. An equilibrium  $\xi \in \mathbb{R}^n$  of (1) satisfies  $f(\xi) = 0$ . We begin by giving a number of definitions; these are all standard in the literature, see for example [3, 5].

**Definition 2.1**  $\phi_j(t)$  is a *heteroclinic orbit* between two equilibria  $\xi_j$  and  $\xi_{j+1}$  of (1) if  $\phi_j(t)$  is a solution of (1) which is backward asymptotic to  $\xi_j$  and forward asymptotic to  $\xi_{j+1}$ .

**Definition 2.2** A *heteroclinic cycle* is an invariant set  $X \subset \mathbb{R}^n$  consisting of the union of a set of equilibria  $\{\xi_1, \dots, \xi_m\}$  and orbits  $\{\phi_1, \dots, \phi_m\}$ , where  $\phi_j$  is a heteroclinic orbit between  $\xi_j$  and  $\xi_{j+1}$ ; and  $\xi_{m+1} \equiv \xi_1$ . We require that  $m \geq 2$ .

We will often take subscripts and similar objects to be modulo  $m$  when it is clear to do so. In order to define robust heteroclinic cycles, recall that for  $x \in \mathbb{R}^n$  the *isotropy subgroup*  $\Sigma_x$  is

$$\Sigma_x = \{\sigma \in \Gamma : \sigma x = x\},$$

and for  $\Sigma$  an isotropy subgroup of  $\Gamma$ , the *fixed-point subspace*  $\text{Fix } \Sigma$  is

$$\text{Fix } \Sigma = \{x \in \mathbb{R}^n : \sigma x = x \ \forall \sigma \in \Sigma\}.$$

**Definition 2.3** A heteroclinic cycle  $X$  is *robust* if for each  $j$ ,  $1 \leq j \leq m$ , there exists a fixed-point subspace,  $P_j = \text{Fix } \Sigma_j$  where  $\Sigma_j \subset \Gamma$  and

- (i)  $\xi_j$  is a hyperbolic saddle and  $\xi_{j+1}$  is a hyperbolic sink for the flow restricted to  $P_j$ ,
- (ii) there is a heteroclinic connection from  $\xi_j$  to  $\xi_{j+1}$  contained in  $P_j$ .

Importantly, robust heteroclinic cycles may occur as codimension-zero phenomena in systems with symmetry. That is, they may exist for open sets of parameter values. We define  $L_j \equiv P_{j-1} \cap P_j$  and clearly  $\xi_j \in L_j$ . Following [4], the eigenvalues of the linearisation of  $f(x)$  about each equilibrium can be classified according to the subspaces in which the eigenspaces lie, as shown in table 1.

Krupa and Melbourne [5] classify cycles in  $\mathbb{R}^4$  and higher dimensions into Types A, B and C. In this paper, we are interested in cycles of Type C:

**Definition 2.4** A heteroclinic cycle  $X$  is of *Type C* if for each  $j$ ,  $1 \leq j \leq m$ ,

Table 1. Classification of eigenvalues.  $P \ominus L$  denotes the orthogonal complement in  $P$  of the subspace  $L$ .

Eigenvalue class	Subspace
Radial ( $r$ )	$L_j \equiv P_{j-1} \cap P_j$
Contracting ( $c$ )	$V_j(c) = P_{j-1} \ominus L_j$
Expanding ( $e$ )	$V_j(e) = P_j \ominus L_j$
Transverse ( $t$ )	$V_j(t) = (P_{j-1} + P_j)^\perp$

there exist fixed point subspaces  $Q_j$  and  $R_j$  such that

$$Q_j = P_j \oplus V_j(c) = P_j \oplus V_{j+1}(t),$$

$$R_j = P_j \oplus V_j(t) = P_j \oplus V_{j+1}(e).$$

Geometrically, we can interpret this as saying that the contracting direction at  $\xi_j$  is the same as the transverse direction at  $\xi_{j+1}$ , and that the transverse direction at  $\xi_j$  is the same as the expanding direction at  $\xi_{j+1}$ .

Conditions for asymptotic stability of heteroclinic cycles can be quite complicated [5, 15], but a necessary condition is that all transverse eigenvalues have negative real part. A *transverse bifurcation* occurs when the cycle loses asymptotic stability as the real part of a transverse eigenvalue passes through zero [20]. Conditions for resonance bifurcations are more complicated [5, 15] and often result in the birth or death of a branch of long-period periodic orbits. We discuss resonance bifurcations from specific cycles in more detail below.

Heteroclinic cycles which are not asymptotically stable can still have strong attractivity properties. The following definition is from Melbourne [21].

**Definition 2.5** An invariant set  $X$  is *essentially asymptotically stable (e.a.s.)* if there exists a set  $\mathcal{A}$  such that given any real number  $a \in (0, 1)$ , and any neighbourhood  $\mathcal{U}$  of  $X$ , there is an open neighbourhood  $\mathcal{V} \subset \mathcal{U}$  of  $X$  such that:

- (i) all trajectories starting in  $\mathcal{V} \setminus \mathcal{A}$  remain in  $\mathcal{U}$  and are asymptotic to  $X$ ,
- (ii)  $\mu(\mathcal{V} \setminus \mathcal{A})/\mu(\mathcal{V}) > a$ , where  $\mu$  is Lebesgue measure.

Essential asymptotic stability of heteroclinic cycles often arises when, due to an unstable transverse eigenvalue, there is a cusp-shaped region of points abutting the cycle which is not attracted to the cycle.

## 2.2 Type C heteroclinic cycles

We now describe in more detail the Type C heteroclinic cycles that we study in this paper. We consider a system of ordinary differential equations,  $\dot{x} = f(x)$ , where  $x = (x_1, x_2, x_3, x_4) \in \mathbb{R}^4$  and  $f : \mathbb{R}^4 \rightarrow \mathbb{R}^4$  is a  $\mathbf{C}^1$  vector-valued function. We assume this system is  $\Gamma$ -equivariant, that is

$$\gamma(f(x)) = f(\gamma(x)), \quad \forall \gamma \in \Gamma,$$

where the group  $\Gamma$  is given by

$$\Gamma = \Lambda \ltimes \mathbb{Z}_2^4.$$

We take one of two choices for  $\Lambda$ , as described below. The  $\mathbb{Z}_2^4$  subgroup is generated by the following elements:

$$\kappa_1 : (x_1, x_2, x_3, x_4) \rightarrow (-x_1, x_2, x_3, x_4),$$

$$\kappa_2 : (x_1, x_2, x_3, x_4) \rightarrow (x_1, -x_2, x_3, x_4),$$

$$\kappa_3 : (x_1, x_2, x_3, x_4) \rightarrow (x_1, x_2, -x_3, x_4),$$

$$\kappa_4 : (x_1, x_2, x_3, x_4) \rightarrow (x_1, x_2, x_3, -x_4).$$

These symmetries ensure the existence of dynamically invariant subspaces in which robust saddle–sink connections can occur. We later consider three cases for the symmetries and eigenvalue structure of the heteroclinic cycle. In case 1,  $\Lambda = \mathbb{Z}_4$ , and is generated by the element

$$\rho_1 : (x_1, x_2, x_3, x_4) \rightarrow (x_2, x_3, x_4, x_1).$$

In cases 2 and 3,  $\Lambda = \mathbb{Z}_2$ , and is generated by the element

$$\rho_2 : (x_1, x_2, x_3, x_4) \rightarrow (x_3, x_4, x_1, x_2).$$

In all cases, we assume that there are four saddle-type equilibria lying on the coordinate axes, which we label  $\xi_1, \dots, \xi_4$ . Within each two-dimensional subspace  $P_j = \{x \in \mathbb{R}^4 \mid x_{j+2} = x_{j+3} = 0\}$ , we assume there is a heteroclinic connection connecting  $\xi_j$  with  $\xi_{j+1}$ .

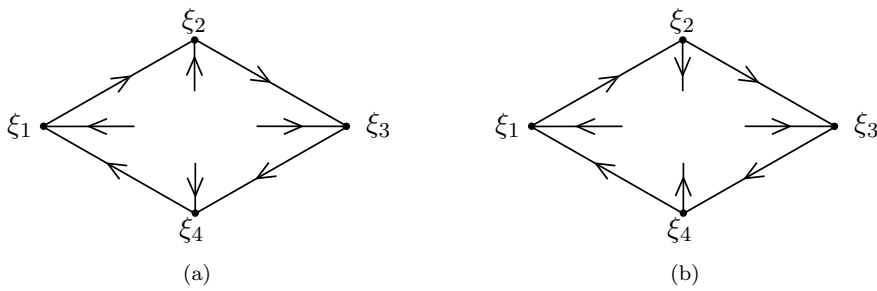


Figure 1. Schematic diagrams of the Type C cycles we consider. In (a), all transverse eigenvalues are negative, corresponding to cases 1 and 2. In (b),  $\xi_1$  and  $\xi_3$  have negative transverse eigenvalues and  $\xi_2$  and  $\xi_4$  have positive transverse eigenvalues, corresponding to case 3.

We assume all equilibria have real eigenvalues. Each equilibrium  $\xi_j$  has one radial eigenvalue,  $-r_j < 0$ , one contracting eigenvalue  $-c_j < 0$ , one expanding eigenvalue  $e_j > 0$  and one transverse eigenvalue  $-t_j$ . We allow for positive or negative transverse eigenvalues. In cases 1 and 2, all transverse eigenvalues are negative. In case 3,  $\xi_1$  and  $\xi_3$  have negative transverse eigenvalues, but  $\xi_2$  and  $\xi_4$  have positive transverse eigenvalues. Schematics of the cycles in each case are shown in figure 1. In the notation of [5], the cycle in case 1 is of type  $C_1^-$ , and the cycle in cases 2 and 3 is of type  $C_2^-$ .

### 2.3 Poincaré maps

In this section we describe the construction of the Poincaré maps required for modelling the dynamics near the heteroclinic cycle, via the composition of local and global maps in the usual way. We describe the details only for the flow near  $\xi_1$ , in case 1, where the equilibria are related by the  $\mathbb{Z}_4$  symmetry, and all transverse eigenvalues are negative. The details near the other equilibria and in the other cases are very similar.

We assume that the flow can be linearised about  $\xi_1$ , and that the local linearised flow near  $\xi_1$  is

$$\dot{u}_1 = -r_1 u_1, \tag{2a}$$

$$\dot{x}_2 = e_1 x_2, \tag{2b}$$

$$\dot{x}_3 = -t_1 x_3, \tag{2c}$$

$$\dot{x}_4 = -c_1 x_4, \tag{2d}$$

where  $u_1$  is a local radial coordinate which is zero at  $\xi_1$ . At  $\xi_1$ ,  $x_2$ ,  $x_3$  and  $x_4$  are respectively the expanding, transverse and contracting coordinates. We define cross sections

$$H_1^{\text{in}} \equiv \{(u_1, x_2, x_3, x_4) \mid |u_1| < h, 0 \leq x_2, x_3 < h, x_4 = h\},$$

$$H_1^{\text{out}} \equiv \{(u_1, x_2, x_3, x_4) \mid |u_1| < h, x_2 = h, 0 \leq x_3, x_4 < h\},$$

near  $\xi_1$ , and

$$H_2^{\text{in}} \equiv \{(x_1, u_2, x_3, x_4) \mid |u_2| < h, 0 \leq x_3, x_4 < h, x_1 = h\},$$

near  $\xi_2$ , so  $H_2^{\text{in}} = \rho_1^{-1} H_1^{\text{in}}$ . The coordinates  $x_1$ ,  $x_3$  and  $x_4$  near  $\xi_2$  are respectively contracting, expanding and transverse, and  $u_2$  is a local radial coordinate which is zero at  $\xi_2$ .

The local flow near  $\xi_1$  induces a map  $\phi_1 : H_1^{\text{in}} \rightarrow H_1^{\text{out}}$ , which is given by:

$$\phi_1(u_1, x_2, x_3, h) = \left( u_1 \left( \frac{x_2}{h} \right)^{\frac{r_1}{e_1}}, h, x_3 \left( \frac{x_2}{h} \right)^{\frac{t_1}{e_1}}, h \left( \frac{x_2}{h} \right)^{\frac{e_1}{e_1}} \right).$$

We construct a global map  $\Phi_{12} : H_1^{\text{out}} \rightarrow H_2^{\text{in}}$  to approximate the dynamics near the heteroclinic connection between  $\xi_1$  and  $\xi_2$ . The heteroclinic connection intersects  $H_1^{\text{out}}$  at  $(u_1, x_2, x_3, x_4) = (0, h, 0, 0)$  and intersects  $H_2^{\text{in}}$  at  $(x_1, u_2, x_3, x_4) = (h, \epsilon_2, 0, 0)$  for a small constant  $\epsilon_2$ . Using the invariance of the coordinate hyperplanes, we can write down the global map to leading order as:

$$\Phi_{12}(u_1, h, x_3, x_4) = (h, \epsilon_2, A_3 x_3, A_4 x_4),$$

where  $A_3$  and  $A_4$  are order 1 positive constants.

We can use the symmetry  $\rho_1$  to construct a return map once around the entire cycle back to  $H_1^{\text{in}}$ . This map is given by  $(\rho_1 \Phi_{12} \phi_1)^4$ . We can thus investigate the dynamics by considering only the map  $\psi = \rho_1 \Phi_{12} \phi_1$ .

If  $r_1 > e_1$  then the  $u_1$  component is contracting, and hence can be ignored. We henceforth assume this is the case. In addition, the lowest order terms in  $\Phi_{12}$  are independent of  $u_1$ , so it is clear that it is only the  $x_3$  and  $x_4$  components that are important for the dynamics [4, 5]. We can thus consider

the two-dimensional map:

$$\psi(x_2, x_3) = (A_3 h^{-\frac{t_1}{e_1}} x_3 x_2^{\frac{t_1}{e_1}}, A_4 h^{1-\frac{c_1}{e_1}} x_2^{\frac{c_1}{e_1}}) \tag{3}$$

The fixed point at the origin in this map corresponds to the heteroclinic cycle in the flow, so we can analyse the stability of the cycle in the flow by analysing the stability of this fixed point in the map. We can rescale the parameters so that  $e_1 = 1$ , which is equivalent to rescaling time in the local equations (2). Except in the case that  $t_1 + c_1 = e_1$ , we can also rescale the coordinates so that  $A_3 h^{-\frac{t_1}{e_1}} = A_4 h^{1-\frac{c_1}{e_1}} = 1$ .

The next section is devoted to the analysis of these maps.

### 3 Analysis of Poincaré maps

In this section we consider three heteroclinic cycles, as described in section 2.2, and investigate their stability by analysing the appropriate Poincaré maps. The three cases we consider are as follows. For the first two cases, all equilibria have negative transverse eigenvalues. In case 1,  $\Lambda = \mathbb{Z}_4$ , and in case 2,  $\Lambda = \mathbb{Z}_2$ . We discuss resonant bifurcations from these cycles in section 3.1 below. The third case we consider has  $\Lambda = \mathbb{Z}_2$ ;  $\xi_1$  and  $\xi_3$  have negative transverse eigenvalues, but  $\xi_2$  and  $\xi_4$  have positive transverse eigenvalues. It is in this case that we find a new mechanism for stability loss.

In each case, the Poincaré map from a section  $H_j^{\text{in}}$  to  $H_{j+1}^{\text{in}}$  is given by a rescaled version of (3), of the form

$$\psi_j : \begin{pmatrix} x \\ y \end{pmatrix} \rightarrow \begin{pmatrix} yx^{t_j} \\ x^{c_j} \end{pmatrix}.$$

Note that this rescaling can only be done away from points of resonance; for  $\psi_j$ , the rescaling required that  $c_j + t_j \neq 1$ . In the following, we only give results that are valid away from resonance. If  $t_j > 0$  we say the transverse direction is stable, and if  $t_j < 0$  we say that the transverse direction is unstable. We always have  $c_j > 0$ . For each map, we consider the domain to be  $\Sigma = [0, 1) \times [0, 1)$ . Note that  $\psi_j(1, 1) = (1, 1)$ , for all  $c_j$  and  $t_j$ . In the following analysis, in order to understand how points move under the action of maps such as  $\psi_j$ , we frequently consider the image of a curve  $y = x^a$  (which passes through

(1, 1)). This allows us to reduce the two-dimensional Poincaré maps to a one-dimensional map acting on the exponents ( $a$ ) of these curves.

### 3.1 Cases 1 and 2: resonance bifurcations

In this section we recall some results of Krupa and Melbourne [5] regarding the stability of Type C cycles with stable transverse directions. We consider the dynamics of the maps in more detail than they do, which helps with the analysis of the new bifurcation in the following section.

In case 1,  $\Lambda = \mathbb{Z}_4$ . The stability of the cycle can be determined by computing the stability of the zero solution in the map

$$\psi_1 : \begin{pmatrix} x \\ y \end{pmatrix} \rightarrow \begin{pmatrix} yx^{t_1} \\ x^{c_1} \end{pmatrix}. \quad (4)$$

As shown by Krupa and Melbourne, the cycle is asymptotically stable if and only if  $t_1 + c_1 > 1$ . Breaking this condition results in a resonant bifurcation.

In case 2,  $\Lambda = \mathbb{Z}_2$ , the Poincaré maps near alternate equilibria are different, so we have to consider the composition of the two maps  $\psi_1$  and  $\psi_2$ :

$$\psi_1 : \begin{pmatrix} x \\ y \end{pmatrix} \rightarrow \begin{pmatrix} yx^{t_1} \\ x^{c_1} \end{pmatrix}, \quad \psi_2 : \begin{pmatrix} x \\ y \end{pmatrix} \rightarrow \begin{pmatrix} yx^{t_2} \\ x^{c_2} \end{pmatrix}.$$

Starting on  $H_1^{\text{in}}$ , the map describing the dynamics of one full circuit around the cycle is:

$$\psi_{21} = \psi_2 \circ \psi_1 : \begin{pmatrix} x \\ y \end{pmatrix} \rightarrow \begin{pmatrix} x^{c_1+t_1t_2} y^{t_2} \\ x^{t_1c_2} y^{c_2} \end{pmatrix}. \quad (5)$$

Krupa and Melbourne [5] show that the zero solution of this map is asymptotically stable if and only if

$$c_1 + c_2 + t_1t_2 > \min(2, 1 + c_1c_2). \quad (6)$$

We now make the following further observations of the dynamics of these maps, which help us to understand the new bifurcation we describe in section 3.2.

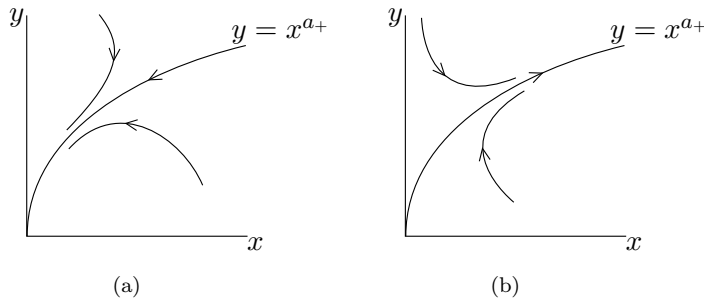


Figure 2. Schematic of the dynamics of points near the origin in the (second iterate of the) map (4), before and after the resonance bifurcation. Successive points are joined with a smooth line only for clarity, of course, the figure depicts a map, not a flow. In (a)  $c_1 + t_1 > 1$ , in (b)  $c_1 + t_1 < 1$ .

First consider the map  $\psi_1$  in (4). The image of a curve  $y = x^a$  under  $\psi_1$  is  $y = x^{h(a)}$  where

$$h(a) = \frac{c_1}{a + t_1}. \tag{7}$$

The map  $h$  has fixed points at

$$a = a_{\pm} \equiv \frac{-t_1 \pm \sqrt{t_1^2 + 4c_1}}{2},$$

where  $a_- < 0 < a_+$ . Thus the curves  $y = x^{a_{\pm}}$  are invariant under the map  $\psi_1$ . Since  $a_+$  is an attracting fixed point in  $h$ , the curve  $y = x^{a_+}$  will be attracting in the map  $\psi_1$ . The basin of attraction of  $a_+$  under  $h$  includes the region  $[0, \infty)$ , and so all points  $(x, y) \in \Sigma$  will move towards the curve  $y = x^{a_+}$  under iteration of  $\psi_1$ .

On the curve  $y = x^{a_+}$ , the dynamics of the map is  $y \rightarrow y^{c_1/a_+}$ , and it can easily be computed that if  $c_1 + t_1 > 1$ , then  $c_1/a_+ > 1$ , and so  $y$  decreases along trajectories. If  $c_1 + t_1 < 1$ , then  $c_1/a_+ < 1$ , and so  $y$  increases along trajectories. This transition is shown schematically in figure 2. Note that since under a single iterate of (4), points cross from one side of the curve  $y = x^{a_+}$  to the other, for clarity, figure 2 shows the dynamics under the second iterate of the map.

We can perform similar computations for the map  $\psi_{21}$  in (5). The curve

$y = x^b$  maps to  $y = x^{g(b)}$  under  $\psi_{21}$ , where

$$g(b) = \frac{c_2(t_1 + b)}{c_1 + t_2(t_1 + b)}. \tag{8}$$

The map  $g$  has fixed points at

$$b = b_{\pm} \equiv \frac{c_2 - c_1 - t_1 t_2 \pm \sqrt{(c_2 - c_1 - t_1 t_2)^2 + 4t_1 t_2 c_2}}{2t_2}, \tag{9}$$

where  $b_- < 0 < b_+$ , and it can be shown that  $b_+$  is a stable fixed point of  $g$ , with a domain of attraction including  $[0, \infty)$ .

Thus, the map  $\psi_{21}$  (5) has invariant curves  $y = x^{b_{\pm}}$ , and the curve  $y = x^{b_+}$  is attracting, in that all points in  $\Sigma$  move towards it, under the action of  $\psi_{21}$ . It can easily be computed that if (6) holds, then the dynamics on the invariant curve  $y = x^{b_+}$  is such that trajectories move towards the origin. If  $c_1 + c_2 + t_1 t_2 < \min(2, 1 + c_1 c_2)$ , then trajectories move away from the origin. By continuity, points on curves close to  $y = x^{b_+}$  will also move towards or away from the origin. The change in dynamics at the transition is a resonant bifurcation, and schematically is similar to that shown in figure 2.

If we allow the  $t_j$  to be negative, then  $b_{\pm}$  may not exist in  $\mathbb{R}$ . In the case where one or more of the  $t_j$  are negative, and the  $b_{\pm}$  are real, then the conditions giving the dynamics along the invariant curves are unchanged. That is, the conditions for ‘resonance’ bifurcations of the heteroclinic cycles are the same.

We discuss these cases in detail in the following section.

### 3.2 Case 3: a new mechanism for stability loss

We now consider the case where  $\xi_1$  and  $\xi_3$  have stable transverse directions, but  $\xi_2$  and  $\xi_4$  have unstable transverse directions. We set  $\Lambda = \mathbb{Z}_2$ . The cycle is not asymptotically stable, but it can be e.a.s. We include a discussion of conditions for when the cycle is e.a.s. at the end of this section.

We first make the following definitions:

Definition 3.1

$$\begin{aligned} \Sigma_\beta &\equiv \{(x, y) \in \Sigma | y < x^\beta\}, \\ \hat{\Sigma}_\beta &\equiv \{(x, y) \in \Sigma | y > x^\beta\}, \\ L_\beta &\equiv \{(x, y) \in \Sigma | y = x^\beta, (x, y) \neq (0, 0)\}. \end{aligned}$$

We again use the two maps

$$\psi_1 : \begin{pmatrix} x \\ y \end{pmatrix} \rightarrow \begin{pmatrix} yx^{t_1} \\ x^{c_1} \end{pmatrix}, \quad \psi_2 : \begin{pmatrix} x \\ y \end{pmatrix} \rightarrow \begin{pmatrix} yx^{-t_3} \\ x^{c_2} \end{pmatrix},$$

where we have written  $t_2 = -t_3$ , so that  $t_3 > 0$ . The domain of  $\psi_1$  is  $\Sigma$ , and the range is  $\hat{\Sigma}_{\frac{c_1}{t_1}}$ . The domain of  $\psi_2$  is  $\hat{\Sigma}_{t_3}$  and the range is  $\Sigma$ . For the remainder of this paper, we assume that

$$c_1 > t_1 t_3. \tag{10}$$

This ensures that the domain of  $\psi_2$  only includes points which are in the range of  $\psi_1$ . That is, there are no trajectories being included in the map which did not originally pass through  $H_1^{\text{in}}$ .

We consider the map  $\psi_A = \psi_2 \circ \psi_1$ :

$$\psi_A : \begin{pmatrix} x \\ y \end{pmatrix} \rightarrow \begin{pmatrix} x^{c_1 - t_1 t_3} y^{-t_3} \\ x^{t_1 c_2} y^{c_2} \end{pmatrix}. \tag{11}$$

Note that if (10) is not satisfied then for all  $(x, y) \in \Sigma$  the  $x$ -component of  $\psi_A(x, y)$  is greater than 1, and hence the origin is completely unstable.

We now state our main result for this section. Given certain conditions on the eigenvalues, we show that a subset of  $\Sigma$  remains in  $\Sigma$  under iteration of  $\psi_A$ , and trajectories move towards the origin. Other points in  $\Sigma$  are shown to leave  $\Sigma$  after a finite number of iterations of  $\psi_A$ .

THEOREM 3.2 *Let*

$$\beta_+ = \frac{c_1 - c_2 - t_1 t_3 + \sqrt{(c_1 - c_2 - t_1 t_3)^2 - 4c_2 t_1 t_3}}{2t_3}.$$

(i) If all three of the following conditions on parameters hold:

$$c_1 - c_2 - t_1 t_3 > 0, \tag{12}$$

$$(c_1 - c_2 - t_1 t_3)^2 - 4c_2 t_1 t_3 > 0, \tag{13}$$

$$c_1 + c_2 - t_1 t_3 > \min(2, 1 + c_1 c_2), \tag{14}$$

then

a) for all  $(x, y) \in \Sigma_{\beta_+}$  there exists some  $N > 0$  such that  $\psi_A^N(x, y) \notin \Sigma$ .

b) for all  $(x, y) \in \hat{\Sigma}_{\beta_+}$ ,  $\psi_A^N(x, y) \in \Sigma$  for all  $N > 0$ , and  $\psi_A^N(x, y) \rightarrow (0, 0)$  as  $N \rightarrow \infty$ .

(ii) If (12) and (13) hold but

$$c_1 + c_2 - t_1 t_3 < \min(2, 1 + c_1 c_2), \tag{15}$$

then (i)a) still holds but for  $(x, y) \in \hat{\Sigma}_{\beta_+}$ ,  $\psi_A^N(x, y) \not\rightarrow (0, 0)$  as  $N \rightarrow \infty$ .

(iii) If either of the following hold:

$$c_1 - c_2 - t_1 t_3 < 0, \tag{16}$$

$$(c_1 + c_2 - t_1 t_3)^2 - 4c_1 c_2 < 0, \tag{17}$$

then for all  $(x, y) \in \Sigma$  there exists some  $N > 0$  such that  $\psi_A^N(x, y) \notin \Sigma$ .

*Proof* The image of a curve  $y = x^\beta$  under  $\psi_A$  is  $y = x^{g(\beta)}$ , where

$$g(\beta) = \frac{c_2(t_1 + \beta)}{c_1 - t_3(t_1 + \beta)}, \quad \beta \neq \beta_1 \equiv \frac{c_1}{t_3} - t_1 > 0. \tag{18}$$

The image of the curve  $y = x^{\beta_1}$  is the line  $x = 1$ . Note that, for all parameter values, if  $(x, y) \in \Sigma_{\beta_1} \cup L_{\beta_1}$ , then  $\psi_A(x, y) \notin \Sigma$ .

We now begin by proving (i). Assume that (12), (13) and (14) all hold. Then the map  $g$  has fixed points at

$$\beta_{\pm} = \frac{c_1 - c_2 - t_1 t_3 \pm \sqrt{(c_1 - c_2 - t_1 t_3)^2 - 4c_2 t_1 t_3}}{2t_3},$$

where  $\beta_+ > \beta_- > 0$  (and  $\beta_{\pm} = b_{\mp}$ ). A sketch of  $g$  is shown in figure 3, and it is clear that  $\beta_-$  is a stable fixed point of the map  $g$ , and  $\beta_+$  is an unstable fixed point. Note also that if  $\beta_0 \in [0, \beta_+)$  then  $g^N(\beta_0) \rightarrow \beta_-$  as  $N \rightarrow \infty$ , and

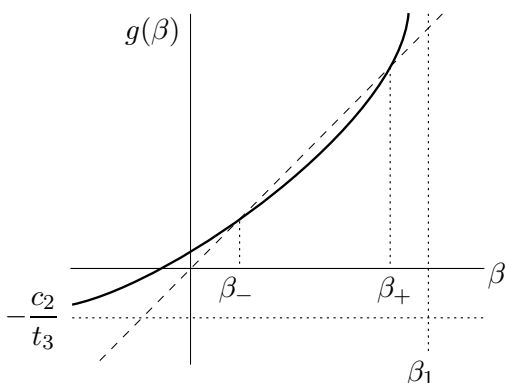


Figure 3. Sketch of the map  $g$  as given in (18).

if  $\beta_0 \in (\beta_+, \beta_1)$  then there exists some  $N > 0$  for which  $g^N(\beta_0) > \beta_1$ . We use this information to deduce the following properties of  $\psi_A$ .

Firstly, if  $(x, y) \in \Sigma_{\beta_+} \setminus (\Sigma_{\beta_1} \cup L_{\beta_1})$ , then there exists some  $N$  for which  $\psi_A^{N-1}(x, y) \in \Sigma_{\beta_1}$ . Hence  $\psi_A^N(x, y) \notin \Sigma$ .

Secondly, for  $(x, y) \in \hat{\Sigma}_{\beta_+}$ ,  $\psi_A^N(x, y) \rightarrow L_{\beta_-}$  as  $N \rightarrow \infty$ . The dynamics on  $y = x^{\beta_-}$  is the same as the dynamics on the curve  $y = x^{\beta_+}$ , as computed in section 3.1. That is, since (14) holds, trajectories on  $y = x^{\beta_-}$  move towards the origin. Hence  $\psi_A^N(x, y) \rightarrow (0, 0)$  as  $N \rightarrow \infty$ .

We next prove (ii). The dynamics for points starting in  $\Sigma_{\beta_+}$  are unchanged. But since (15) holds, trajectories on  $y = x^{\beta_-}$  move away from the origin, and so for  $(x, y) \in \hat{\Sigma}_{\beta_+}$ ,  $\psi_A^N(x, y)$  moves away from the origin as  $N \rightarrow \infty$ .

Finally, we prove (iii). If (17) holds, then there are no fixed points in the map  $g$ . If (16) holds, then  $\beta_{\pm} < 0$ . In both cases, for all  $\beta_0 \in [0, \beta_1)$ , then there exists some  $N > 0$  for which  $g^N(\beta_0) > \beta_1$ . Hence, for all  $(x, y) \in \Sigma \setminus (\Sigma_{\beta_1} \cup L_{\beta_1})$ , there exists some  $N$  for which  $\psi_A^{N-1}(x, y) \in \Sigma_{\beta_1}$ , and so  $\psi_A^N(x, y) \notin \Sigma$ . □

The dynamics on the curve  $y = x^{\beta_+}$  can be easily computed, and we find that trajectories move towards the origin along this curve if

$$2 < c_1 + c_2 - t_1 t_3 < 1 + c_1 c_2. \tag{19}$$

The conditions (14) and (19) are the equivalent of resonant bifurcation conditions for this heteroclinic cycle. There will be some differences from the usual resonant bifurcations, because the original cycle is not asymptotically stable,

although it may be e.a.s. We still expect that a long-period periodic orbit will branch from the bifurcation point, although we leave the details of this computation to a later study.

In figure 4(a), we show curves of the equations

$$c_1 + c_2 - t_1 t_3 = 2, \quad (20)$$

$$c_1 + c_2 - t_1 t_3 = 1 + c_1 c_2, \quad (21)$$

$$c_1 - c_2 - t_1 t_3 = 0, \quad (22)$$

$$(c_1 - c_2 - t_1 t_3)^2 = 4c_2 t_1 t_3, \quad (23)$$

in  $c_1$ - $c_2$  space, as these may denote boundaries between different types of behaviour. Curves (20) and (21) are boundaries that may correspond to resonant-type bifurcations. Curves (22) and (23) are boundaries that may correspond to the new mechanism of stability loss. Which regions of the curves are actually stability boundaries depends on the exact arrangement of the curves, as can be seen in figure 4.

Note that the curves (20), (21) and (23) meet at the same point, where  $c_1 c_2 = 1$ , and the curves (21) and (23) are tangent at that point. In figure 4(b), we show only those parts of the curves which form boundaries between regions with different dynamics near the heteroclinic cycle.

In figure 5, we show the dynamics in each region indicated by (a)-(d) in figure 4(b). The new mechanism for stability loss is the transition between regions (c) and (d). Within the map  $g$ , this is a saddle-node bifurcation of the fixed points  $\beta_+$  and  $\beta_-$ . In the map (11), and hence in the flow, the saddle-node type behaviour is evident in the fact that the invariant curves  $y = x^{\beta_+}$  and  $y = x^{\beta_-}$  come together, coalesce and disappear.

**3.2.1 Transient behaviour.** Note that when condition (13) is broken, there is some interesting transient behaviour. The origin in the map  $\psi_A$  is completely unstable, that is, all initial conditions eventually move far away from the origin. However, some trajectories, namely, those which start close to the  $y$ -axis, initially approach the origin, before moving away in the  $x$ -direction. This is shown in figure 5(d). We now give a brief discussion of why the transient behaviour occurs, considering the behaviours of both the map  $g$  and the

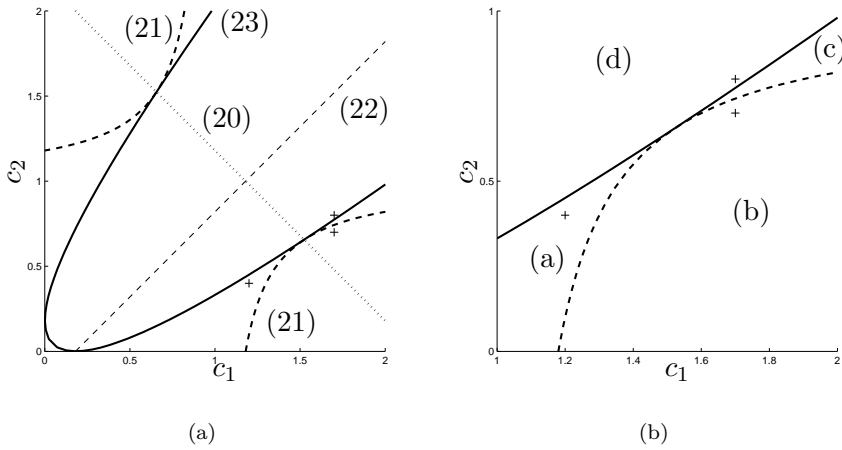


Figure 4. (a) Shows the curves given by equations (20) to (23), in  $c_1$ - $c_2$  parameter space, with  $t_1 = 0.3$  and  $t_3 = 0.6$  (however, the schematic arrangement of the curves is similar for different values of the  $t_j$ ). The dotted line is (20), the thin dashed line is (22), the bold dashed curve is (21) and the solid curve is (23). (b) shows a close up of the bottom-right corner of (a), only showing those curves which form stability boundaries of the heteroclinic cycle. The dynamics in the different regions are shown schematically in figure 5. In regions (b) and (c), the cycle attracts an open set of initial conditions, and depending on the shape of the basin of attraction, the cycle may be e.a.s. In (a) and (d) the cycle is unstable. The + symbols indicate the location in parameter space of the three integrations shown in figures 6, 7, and 8. Note that although (20) does not appear as a stability boundary, being either side of this line is what distinguishes region (a) from region (c).

map  $\psi_A$ , just after the condition (13) has been broken.

Under the map  $g$ , just after the saddle-node bifurcation in which  $\beta_+$  and  $\beta_-$  disappear, trajectories starting with small enough  $\beta$  (which correspond to trajectories under  $\psi_A$  starting with small  $x$ -coordinate) will take a long time to pass through the region where the saddle-node bifurcation took place. During this time, trajectories under  $\psi_A$  move closer to the origin. Eventually, the trajectory of  $\beta$  under  $g$  becomes greater than  $\beta_1$  (given in (18)), and only then does the trajectory under  $\psi_A$  leaves  $\Sigma$ .

This behaviour occurs arbitrarily close to the fixed point at the origin. We give an example of a trajectory showing this transient behaviour in the numerical example section below.

**3.2.2 Conditions for essential asymptotic stability.** For the cycle to be e.a.s., we must at least be in either region (b) or (c) of figure 4. In region (c), we require in addition that  $\beta_+ > 1$ , so that  $\Sigma_{\beta_+}$  is cusp-shaped, and we also

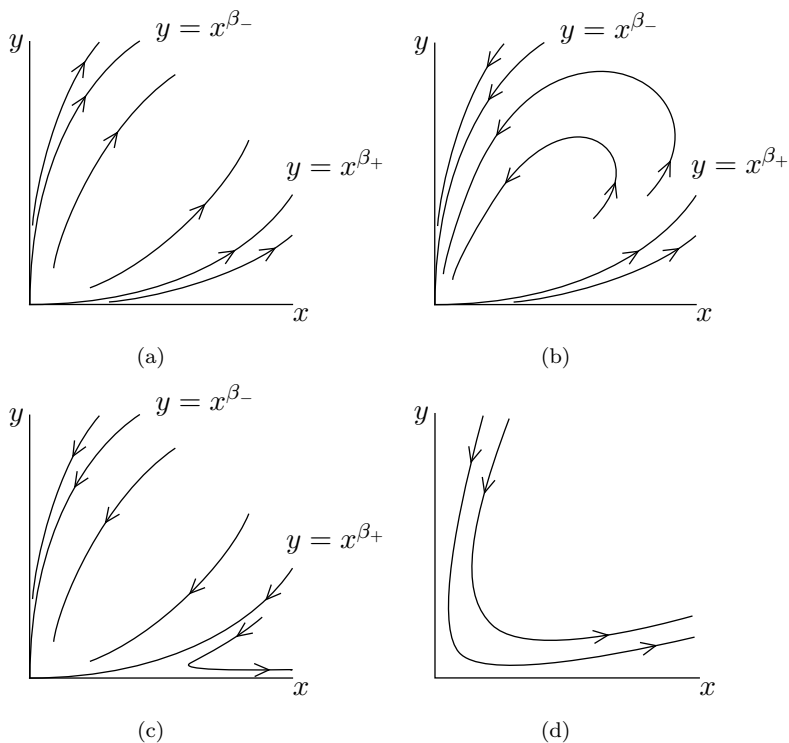


Figure 5. Schematic diagrams showing the dynamics of points near the origin in the map (11), in various regions of parameter space, as indicated in figure 4. In (b) and (c), the cycle attracts an open set of initial conditions, and may be e.a.s., depending on parameters, as described further in the text. In (a) and (d) the cycle is unstable. The new mechanism for change of stability is the transition from (c) to (d).

require that the image of  $\Sigma_{\beta_+}$  under  $\psi_1$  is cusp-shaped. These conditions can be easily computed, and are as follows. For  $\Sigma_{\beta_+}$  to be cusp-shaped, we require

$$c_1 - c_2 - t_1 t_3 > \min(2t_3, c_2 t_1 + t_3). \tag{24}$$

For  $\psi_1(\Sigma_{\beta_+})$  to be cusp-shaped, we require either

$$c_1 - c_2 + t_1 t_3 < 2t_1, \quad \text{or} \quad c_1 - c_2 + t_1 t_3 > c_1 t_3 + t_1. \tag{25}$$

In region (b), the cycle is e.a.s. if both  $\Sigma_{\beta_-}$  and  $\psi_1(\Sigma_{\beta_-})$  are cusp-shaped, conditions for which are:

$$2t_3 < c_1 - c_2 - t_1 t_3 < c_2 t_1 + t_3, \quad \text{and} \quad c_1 - c_2 + t_1 t_3 > \min(2t_1, t_1 + c_1 t_3).$$

If these conditions do not hold, but (24) and (25) do hold, then although ‘essentially all’ trajectories in a neighbourhood of the origin are asymptotic to the origin, most of these will move away from the origin before approaching it, as can be seen in figure 5(b), so the cycle is not e.a.s., although could be termed ‘quasi-essentially asymptotically stable’ (see [23] for another example of this).

We do not mark these regions on figure 4, as they will change as  $t_1$  and  $t_3$  are varied, but note that for the parameters we choose, the heteroclinic cycle is e.a.s. for a large part of region (c).

#### 4 Numerical example

In this section we consider a numerical example to demonstrate the new type of bifurcation described in section 3.2. Recall we have  $\Lambda = \mathbb{Z}_2$ , and  $\xi_1$  and  $\xi_3$  have stable transverse directions, but  $\xi_2$  and  $\xi_4$  have unstable transverse directions.

We consider the equations

$$\dot{x}_1 = x_1(1 - X - c_2x_2^2 - t_1x_3^2 + x_4^2), \quad (26a)$$

$$\dot{x}_2 = x_2(1 - X + x_1^2 - c_1x_3^2 + t_3x_4^2), \quad (26b)$$

$$\dot{x}_3 = x_3(1 - X - t_1x_1^2 + x_2^2 - c_2x_4^2), \quad (26c)$$

$$\dot{x}_4 = x_4(1 - X - c_1x_1^2 + t_3x_2^2 + x_3^2), \quad (26d)$$

where  $X = \sum_{j=1}^4 x_j^2$ , and  $c_1, c_2, t_1, t_3 > 0$  are parameters, and also the eigenvalues at the equilibria as described in section 2.2. The four equilibria  $\xi_j$  lie on the coordinate axes, and there exists a heteroclinic cycle between them of the type described in section 3.2. For numerical integration purposes, we use the transformation  $y_j = \log(x_j)$ , and instead integrate the  $\dot{y}_j$  equations, using a standard RK4 integrator. This improves numerical accuracy as we are able to get very close to the invariant planes with  $x_j = 0$  without having to worry about numerical errors caused by very small variables.

We set  $t_1 = 0.6$  and  $t_3 = 0.3$ . In figure 4, we show the stability region boundaries in  $c_1$ - $c_2$  space. In figures 6, 7, and 8, we show integrations of equations (26) for initial conditions near the heteroclinic cycle in three cases. In

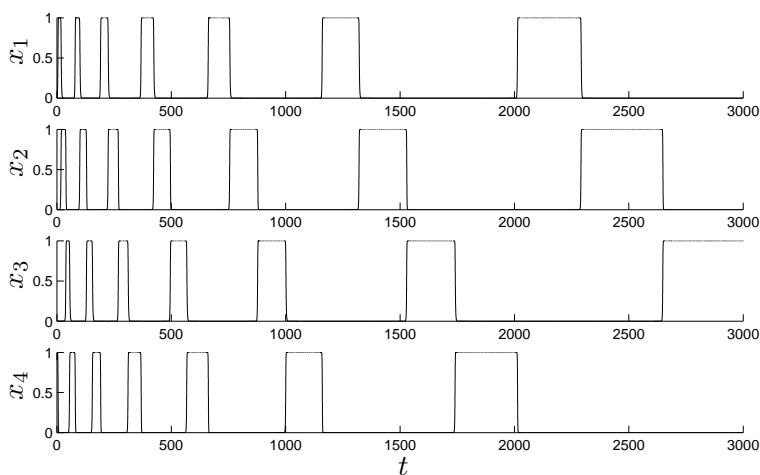


Figure 6. Numerical integration of (26) for a parameter set for which the heteroclinic cycle is attracting. The trajectory spends longer and longer times near each equilibrium. Parameters are  $c_1 = 1.7$ ,  $c_2 = 0.7$ ,  $t_1 = 0.6$ ,  $t_3 = 0.3$ . Initial conditions are  $y(0) = (-5, -15, -10, -0.1)$ .

figure 6 the trajectory shown approaches the cycle. In figure 7, the cycle is resonantly unstable, and solutions move directly away from the cycle, in this case towards a periodic orbit. In figure 8, the cycle is also unstable. The trajectory shown displays the transient behaviour described in section 3.2.1. The trajectory initially approaches the network, indicated by the increasing lengths of time spent near each equilibrium. However, after about  $t = 1500$ , these times start to decrease, and the trajectory moves away from the cycle, in this case eventually asymptoting onto an equilibrium which is not part of the cycle.

## 5 Discussion

In this paper we have investigated a new mechanism of stability loss from a heteroclinic cycle. This mechanism is qualitatively different from previously studied resonant or transverse bifurcations, and is of particular interest because when the cycle is unstable, open sets of initial conditions still move towards the cycle for some time before moving away. Our analysis uses the standard method of constructing linearised Poincaré maps. This reduces a four-dimensional system of differential equations to a two-dimensional map. We study the maps by considering their action on a family of curves, giving

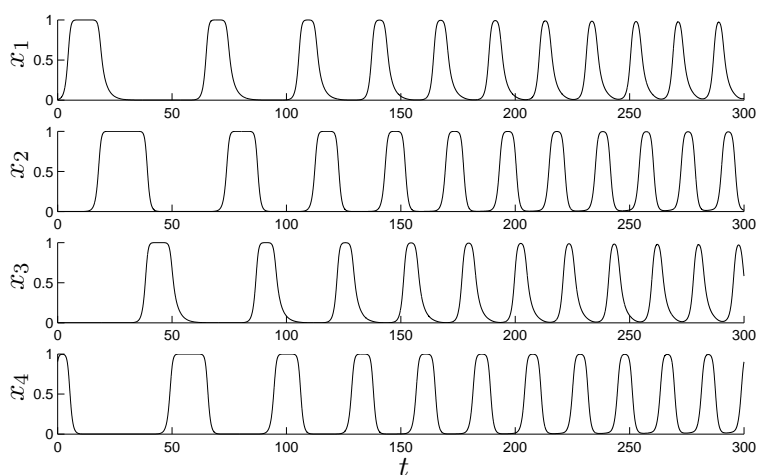


Figure 7. Numerical integration of (26) for a parameter set for which the heteroclinic cycle has undergone a resonant bifurcation. The trajectory moves away from the cycle, towards a periodic orbit. Parameters are  $c_1 = 1.2$ ,  $c_2 = 0.4$ ,  $t_1 = 0.6$ ,  $t_3 = 0.3$ . Initial conditions are  $y(0) = (-5, -15, -10, -0.1)$ .

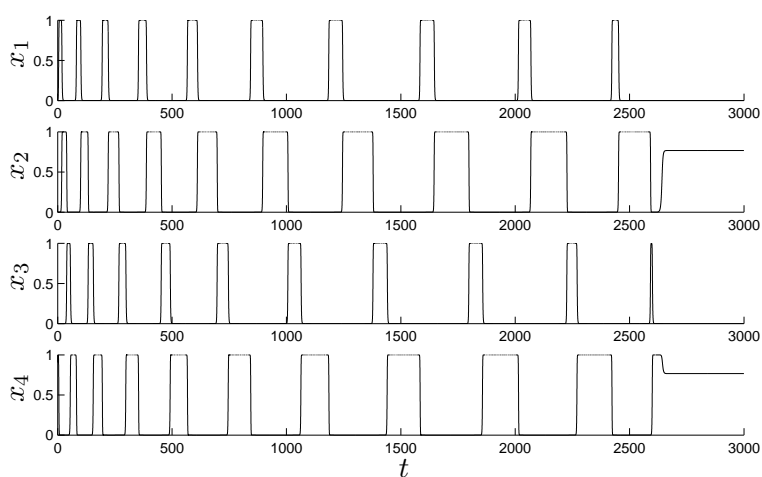


Figure 8. Numerical integration of (26) for a parameter set for which the heteroclinic cycle has undergone the new type bifurcation. The trajectory initially approaches the cycle and spends increasingly long times near the equilibria. Eventually the trajectory starts to move away and leaves a neighbourhood of the cycle, asymptoting onto an equilibrium that is not part of the cycle.

Parameters are  $c_1 = 1.7$ ,  $c_2 = 0.8$ ,  $t_1 = 0.6$ ,  $t_3 = 0.3$ . Initial conditions are  $y(0) = (-5, -15, -10, -0.1)$ .

a further reduction to a one-dimensional map acting on parameters of these curves. We confirm our analysis with a numerical example.

It appears from the analysis and the numerical example that there are no dynamical structures which merge with the cycle at the point of stability loss. This is interesting as it differs from the case of generic bifurcations in which the generation of new structures is associated with changes in stability. We have not ruled out the possibility that some unstable dynamical structure is merging with the cycle in a subcritical bifurcation, but leave a detailed examination of this to a future study.

One current topic of interest in the dynamical systems community is that of ‘switching’ between two or more heteroclinic cycles which are part of a heteroclinic network [23–26]. There are a number of different examples studied in these papers, each with different mechanisms for switching between the subcycles. These include transverse instabilities of the subcycles [23], complex eigenvalues at an equilibrium within the network [24], chaotic dynamics within the nodes of the network [25] and connections formed by transversal intersections of stable and unstable manifolds [26]. It would be interesting to investigate the consequences of embedding a cycle of the type described in this paper into a heteroclinic network, so that it was unstable in the manner described here. This could result in a system which admits switching between subcycles, and it would be interesting to investigate the similarities and differences between this type of switching and those described above. Work on this problem is ongoing.

### Acknowledgements

This work came about after a search for a ‘small’ heteroclinic network with switching behaviour, inspired by discussions with Alastair Rucklidge and Vivien Kirk. The author is very grateful to two anonymous referees for their careful reading of the manuscript and helpful comments on an earlier draft.

### References

- [1] M. Field, *Lectures on bifurcations, dynamics and symmetry*, Pitman Research Notes in Mathematics Vol. 356 London: Longman Scientific and Technical (1996)
- [2] J. Guckenheimer and P. Holmes, *Structurally stable heteroclinic cycles*, Math. Proc. Camb. Phil. Soc. 103 (1988), pp. 189–192.

- [3] M. Krupa, *Robust heteroclinic cycles*, J. Nonlinear Sci. 7 (1997), pp. 129–176.
- [4] M. Krupa and I. Melbourne, *Asymptotic stability of heteroclinic cycles in systems with symmetry*, Ergod. Th. & Dynam. Sys. 15 (1995), pp. 121–147.
- [5] M. Krupa and I. Melbourne, *Asymptotic stability of heteroclinic cycles in systems with symmetry, II*, Proc. Roy. Soc. Edinburgh A 134A (2004), pp. 1177–1197.
- [6] J. Hofbauer, *Heteroclinic Cycles in Ecological Differential Equations*, Tatra Mountains Math. Publ. 4 (1994), pp. 105–116.
- [7] J. Hofbauer and K. Sigmund, *Evolutionary Games and Population Dynamics*, CUP (1998).
- [8] R. May and W. Leonard, *Nonlinear aspects of competition between three species*, SIAM J. Appl. Math. 29 (1975), pp. 243–253.
- [9] M.I. Rabinovich, R. Huerta, P. Varona and V.S. Afraimovich, *Transient cognitive dynamics, metastability and decision making*, PLoS Comp. Biol. 4 (2008).
- [10] M.I. Rabinovich, P. Varona, A.I. Selverston and H.D.I. Abarbanel, *Dynamical principles in neuroscience*, Rev. Mod. Phys. 78 (2006) pp. 1213–1265.
- [11] M. Rabinovich, A. Volkovskii, P. Lecanda, R. Huerta, H.D.I. Abarbanel and G. Laurent, *Dynamical encoding by networks of competing neuron groups: winnerless competition*, Phys. Rev. Lett. 87 (2001), 068102.
- [12] A. Venaille, P. Varona and M. Rabinovich, *Synchronization and coordination of sequences in two neural ensembles*, Phys. Rev. E 71 (2005), 061909.
- [13] M. Aguiar, P. Ashwin, A. Dias, and M. Field, *Robust heteroclinic cycles in coupled cell systems: Identical cells with asymmetric inputs*. Preprint (2009).
- [14] I. Melbourne, P. Chossat and M. Golubitsky, *Heteroclinic cycles involving periodic solutions in mode interactions with  $O(2)$  symmetry*, Proc. Roy. Soc. Edinburgh 113A (1989), pp. 315–345.
- [15] C.M. Postlethwaite and J.H.P. Dawes, *Resonance bifurcations from robust homoclinic cycles*, Nonlinearity 23 (2010), pp. 621–642.
- [16] M. Field and J. Swift, *Stationary bifurcation to limit cycles and heteroclinic cycles*, Nonlinearity 4 (1991), pp. 1001–1043.
- [17] R. Driessse and A.J. Homburg, *Resonance bifurcation from homoclinic cycles*, Journ. Diff. Eq. 246 (2009), pp. 2681–2705.
- [18] C.M. Postlethwaite and J.H.P. Dawes, *A codimension two resonant bifurcation from a heteroclinic cycle with complex eigenvalues*, Dynamical Systems: An International Journal 21(3) (2006), pp. 313–336.
- [19] A. Scheel and P. Chossat, *Bifurcation d'orbites périodiques à partir d'un cycle homocline symétrique*, C. R. Acad. Sci. Paris Ser. I 314 (1992), pp. 49–54.
- [20] P. Chossat, M. Krupa, I. Melbourne and A. Scheel, *Transverse bifurcations of homoclinic cycles* Physica D 100 (1997), pp. 85–100.
- [21] I. Melbourne, *An example of a non-asymptotically stable attractor*, Nonlinearity 4 (1991), pp. 835–844.
- [22] V. Kirk and M. Silber, *A Competition between heteroclinic cycles*, Nonlinearity 7 (1994), pp. 1605–1621.
- [23] C.M. Postlethwaite and J.H.P. Dawes, *Regular and irregular cycling near a heteroclinic network*, Nonlinearity 18 (2005), pp. 1477–1509.
- [24] V. Kirk, E. Lane, C.M. Postlethwaite, A.M. Rucklidge and M. Silber, *A mechanism for switching near a heteroclinic network*, Submitted to Dynamical Systems (2009).
- [25] P. Ashwin, A.M. Rucklidge and R. Sturman, *Two-state intermittency near a symmetric interaction of saddle-node and Hopf bifurcations: a case study from dynamo theory*, Physica D 194 (2004), pp. 30–48.
- [26] M. Aguiar, S. Castro and I. Labouriau, *Dynamics near a heteroclinic network*, Nonlinearity 18 (2005), pp. 391–414.